ELSEVIER

International Journal of Mass Spectrometry 184 (1999) 67–74

International Journal of Mass Spectrometry

Dissociative photoionisation of OCS from threshold to 40.8 eV

S. Morse[a], M. Takahashi[a], J.H.D. Eland[a,*], L. Karlsson[b]

[a] *Physical and Theoretical Chemistry Laboratory, South Parks Road, Oxford OX1 3QZ, UK*
[b] *Physics Institute, Uppsala University, Box 530, S-751-21 Uppsala, Sweden*

Received 22 September 1998; accepted 5 November 1998

Abstract

Energy-analysed photoelectrons have been measured in coincidence with product ions from photoionisation of carbonyl sulphide at 21.21 and 40.8 eV photon energy. Yields of the different products and kinetic energy release distributions in fragment ion formation are reported. Results on the states below 20 eV agree with previous work, but our interpretation differs; new data are presented on inner valence states. In dissociation from states in the band at 23 eV there is forward/backward asymmetry in fragment ion direction relative to the electrons, indicating a fast dissociation and possibly identifying the band as a 7σ satellite. (Int J Mass Spectrom 184 (1999) 67–74) © 1999 Elsevier Science B.V.

Keywords: Photoinisation; Photelectron-photoion coincidence; OCS

1. Introduction

In contrast to simple measurement of a photoelectron spectrum or of a photoion yield curve by photoionisation mass spectrometry, photoelectron photoion coincidence (PEPICO) spectroscopy provides direct correlation between the initial state of a molecular ion and the fragments formed when the ion dissociates. The parameters that can be measured as functions of initial ion state include the branching ratios to different products, the kinetic energy release distribution in each fragmentation, and the rates of slow (metastable) decays. In addition, angular correlations between the initial photoelectron direction and the fragment ion direction can be observed and are in principle a rich source of information on the dynamics of the ionisation process [1]. Several examples of anisotropic electron–fragment ion correlations have been found in photoionisation of polyatomic molecules [2–4] and recently for diatomic species [5]; strong effects are observed where the reaction is faster than molecular rotation and where the decay involves purely axial recoil. These conditions are likely to be met in the inner valence states of linear triatomic molecules such as OCS. Asymmetric triatomics are particularly suitable targets in a search for anisotropic electron–ion correlations, because of their lack of inversion symmetry, although the kinetic energy release distributions are broader than in diatomic dissociations, because of the vibrational and rotational excitation of the diatomic product. This makes it almost impossible to detect effects of *alignment* between electron and product ion in experiments of the present design, but effects of *orientation*, where electrons leave preferentially from one end of the molecule, should be

* Corresponding author.

PII S1387-3806(98)14254-9

observable. This paper reports an investigation of the PEPICO spectrum of OCS including all states up to 40 eV in a search for such orientation effects. Clear anisotropy has been found in dissociations following ionisation to just one inner valence band. Previous results on the decay of the outer valence single-hole states are largely confirmed.

The valence orbital configuration of the OCS molecule can be written:

$$6\sigma^2\ 7\sigma^2\ 8\sigma^2\ 9\sigma^2\ 2\pi^4\ 3\pi^4 \qquad {}^1\Sigma^+$$

The outer valence states X, A, B, and C arise from ionisation of a single electron from each of the outermost orbitals. All these states have resolved vibrational structure which has been extensively studied by photoelectron spectroscopy [6–10] and threshold photoelectron spectroscopy [11,12]. Since the line widths are narrow, dissociation from these states is not extremely fast. The inner valence states between 19 and 40 eV are much less well known, and, except for the 19 eV band, are reported only in photoelectron studies [13–16] at low resolution. The 19 eV band is apparently continuous, in common with most inner valence bands, possibly because of rapid dissociation in keeping with the high available energy.

The ionic dissociations of OCS^+ from the outer valence states have been examined before using the PEPICO technique [17,18] and in most detail by threshold PEPICO (TPEPICO) [19]. Hubin-Franskin et al. [19] proposed on the basis of their measurements and calculations that a major pathway for decay from the A and B states involves internal conversion to the ionic ground state surface. Fluorescence emission competes with dissociation from the (000) levels of the *A* state; the lifetime was initially found to have both fast and slow components (100 and 500 ns [20]); later measurements have confirmed only the fast decay, with resolution of the spin–orbit components of the ionic state [21,22]. Predissociation lifetimes of the excited levels of A which do not fluoresce were reported to be relatively long if the bending mode is excited, but unmeasurably short on excitation of stretching modes [22]. No recent measurements on the dissociations of OCS^+ from the *C* state have been reported; almost nothing is known about the dissociation behaviour of the inner valence states.

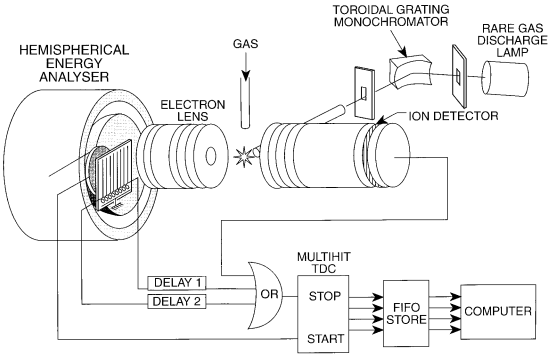

Fig. 1. Scheme of the PEPICO spectrometer. A delay-line encoded position-sensitive detector is located in the focal plane of the hemispherical electron energy analyser.

2. Experimental

The PEPICO spectra of OCS were recorded by using an improved apparatus which is described in detail elsewhere [23] and shown schematically in Fig. 1. Briefly, ions are formed at the intersection of an effusive gas jet with a wavelength-selected light beam from an atomic discharge lamp. Electrons are collected under zero-field conditions by a hemispherical analyser of 125 mm mean radius fitted with a position-sensitive detector. When an electron is detected, a pulsed extraction field is applied to the source and ions are detected in a two-field Wiley–McLaren type [24] time-of-flight (TOF) mass spectrometer. This arrangement allows relatively high mass resolution ($M/\Delta M = 200$) while preserving an electron resolution dependent only on the analyser pass energy. For maximum resolution a pass energy of 5 eV allows peak widths of 50 meV. A complication of the pulsing technique is that a delay is introduced because of the electron flight time between ion formation and extraction. One effect of this delay can be a loss of high-energy light fragment ions, but this is not thought to affect the present data for OCS. The losses and other effects of the delay on peak shapes are accounted for in simulations as part of the data

analysis. To keep the rate of accidental coincidences to below 10% of true coincidences, a level where subtraction is completely reliable, the event rate has to be restricted by low target gas pressure and low light intensity. As a result, the run time for each individual spectrum is about 24 h.

The sample of OCS used was a normal commercial one. It contained small amounts of CO_2 impurity which produced spurious CO^+ and CO_2^+ signals. Since the dissociation characteristics of CO_2 have also been studied [25] these features could be recognised and have been removed in the data analysis.

3. Data reduction

The raw experimental data are a set of individual coincidences linking photoelectron energy and ion flight time. The whole data set can be visualised as a two-dimensional representation; an example of such an intensity-encoded two-dimensional map is shown in Fig. 2. Although all experimental information is included in such a map, it is difficult to use it in this form to draw quantitative conclusions. Most of the analysis is performed on one-dimensional distributions obtained as cuts or projections of the full data set. The most useful of these in determining the sources of the different product ions are photoelectron spectra coincident with individual ions which correspond to vertical cuts around the ion times of flight in the map; several examples are shown in Figs. 3–5. To acquire data on the behaviour of different ionic states, horizontal cuts at fixed electron energy can be taken, giving complete mass spectra arising from the individual electronic state or vibrational level. Peak shapes for single masses in such spectra are interpreted in terms of the kinetic energy release distribution (KERD) in the ion decay.

To analyse ion TOF peak shapes, we use two strategies. Either peak shapes can be transformed into estimated KERDs by direct inversion using smoothing and iterative deconvolution, or the shapes can be compared with simulated peaks in forward convolution. In simulations, effects of anisotropic angular distributions can be included [5], but in direct inversion we assume isotropic distribution of fragment ions.

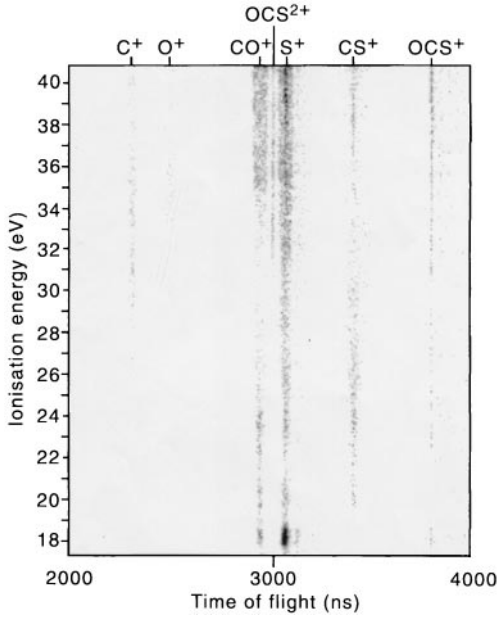

Fig. 2. A two-dimensional spectrum of time of flight vs. ionisation energy for OCS taken at 30.4 nm (40.8 eV photon energy) and at a pass energy of 30 eV. Accidental coincidences have not been subtracted from this image; they account for all the OCS^+ signal visible.

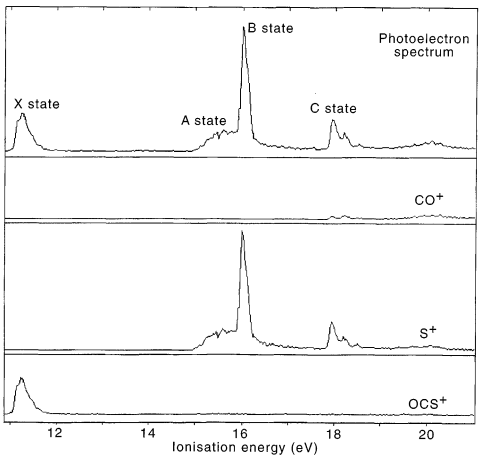

Fig. 3. Photoelectron spectrum and coincident ion spectra of OCS at 58.4 nm (21.2 eV photon energy) and a pass energy of 10 eV. The figure has the same vertical scale from displaced zeros in all parts, with a peak of 900 counts per channel on S^+ from the *B* state.

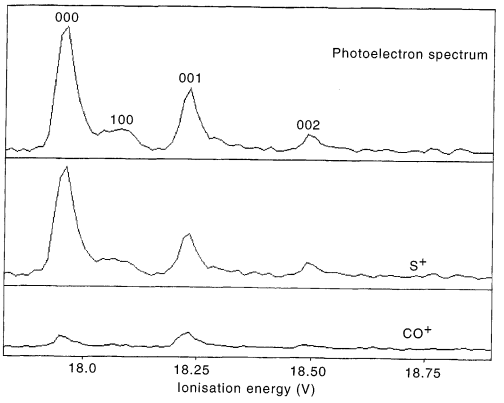

Fig. 4. Detail of photoelectron spectrum and coincident ion spectra for the *C* state of OCS^+ at a pass energy of 5 eV giving about 50 meV resolution. The common vertical scale corresponds to 550 counts per channel at the maximum of the S^+ signal.

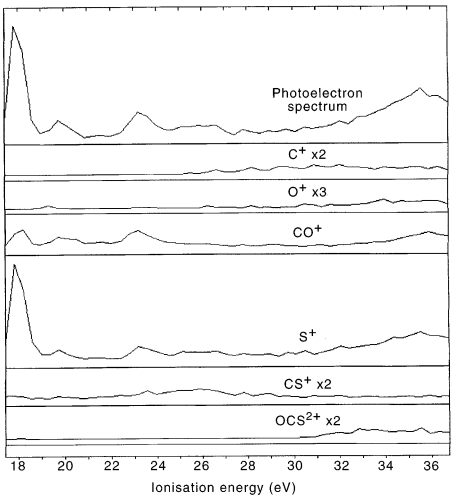

Fig. 5. Photoelectron spectrum and coincident ion spectra in the inner valence region using 30.4 nm radiation and 30 eV pass energy. The signal was 200 counts per channel at the peak for S^+ near 18 eV; for some ions the vertical scale has been expanded as indicated.

4. Results

Photoelectron spectra and coincident photoelectron spectra for different ion products are shown in Figs. 3–5. Examples of ion peak shapes from mass spectra coincident with selected energies or photoelectron bands are shown in Figs. 6 and 7. Three estimates of the KERD for S^+ from OCS^+ [C(000)], obtained from separate experimental runs under different sets of conditions, are shown in Fig. 8 to illustrate the reproducibility of the direct inversion procedure on signals of moderate intensity. The branching ratios are collected in Tables 1 and 2.

4.1. Origin of different ions

The OCS^+ ion remains undissociated only in levels of the ionic ground state below the lowest dissociation limit (Table 3), and in the fraction of the A(000) level which emits fluorescence. The main fragment ion is S^+, which is formed abundantly from all the excited states of OCS^+ populated, and also from OCS^{2+}. From the appearance of the KERDs we believe that S^+ is formed together with CO throughout the energy range, rather than with atomic fragments. The second most abundant ion is CO^+; the formation of this ion starts in the C state, and it continues to be formed from the inner valence states up to 26 eV. It is not formed from the higher inner valence states, but sets in again as a partner to S^+

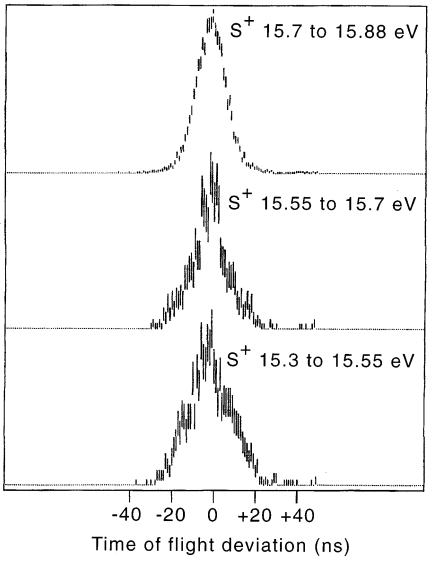

Fig. 6. TOF peak shapes for S^+ fragments coincident with electrons corresponding to the A state of OCS^+, showing normal forward/backward symmetric profiles. The peak S^+ signals in the three spectra were (top to bottom) 900, 100, and 110 counts per channel.

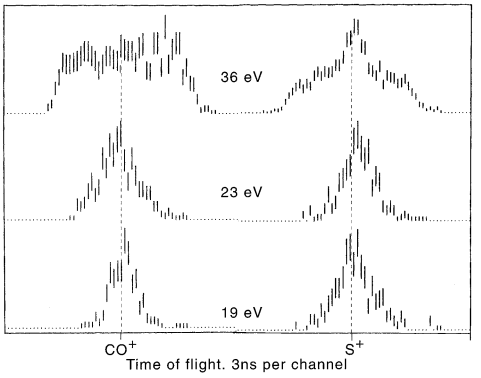

Fig. 7. TOF peaks for S^+ and CO^+ fragment ions coincident with electrons in the 19, 23, and 36 eV ionisation bands. Forward/backward asymmetry is seen as an accumulation of intensity to the right of the centre line for S^+ and to the left of it for CO^+ in the 23 eV band. Maximum signals correspond to about 100 counts per channel in all the peaks.

from dissociative double ionisation above about 34 eV.

The CS^+ ion comes mainly from the inner valence states between 21 and 29 eV, and only with very low abundance from the inner valence state at 19 eV. Its onset is at about 19.5 eV, 1 eV above the first thermodynamic limit for $CS^+ + O$, but below the limits for excited forms of the products.

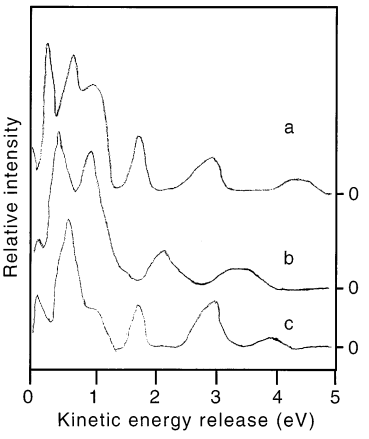

Fig. 8. KERDs derived by direct inversion of the forward halves of TOF peaks coincident with electrons from the *C*(000) level under different conditions: curve (a) 30.4 nm ionisation, 30 V pass energy; curve (b) 58.4 nm ionisation, 10 V pass energy; curve (c) 58.4 nm ionisation, 5 V pass energy. The backward halves of the same peaks give three more independent curves of similar content.

Table 1
Main branching ratios to ionic products from *X*, *A*, *B*, and *C* states of OCS^+

State and vibrational level	% CO^+	% S^+	% OCS^+
X (000)	···	···	100
A (000)	···	78.4 ± 14.6	21.6 ± 7.6
A (100)	···	96.6 ± 12.8	3.4 ± 2.9
A (101)	···	97.9 ± 10.1	2.1 ± 1.5
B (000)	···	100.5 ± 3.0	−0.5 ± 0.4
B (010)	···	98.9 ± 10.5	1.1 ± 1.1
B (100)	···	99.3 ± 8.2	0.7 ± 0.7
C (000)	8.8 ± 0.5	90.0 ± 1.6	1.2 ± 0.3
C (100)	14.7 ± 1.4	84.7 ± 3.5	0.5 ± 0.8
C (001)	22.1 ± 1.4	77.0 ± 2.6	0.8 ± 0.6
C (002)	17.8 ± 1.4	78.3 ± 3.0	3.9 ± 1.0 [a]

[a] The apparent nonzero yield of parent ions is almost certainly an artefact due to scattered electrons.

The C^+ ion is observed only above the atomisation threshold at about 25 eV, where it is first formed with very low kinetic energy. There is thus no detectable formation of $C^+ + SO$. The SO^+ ion is not detected at all, in contrast to the significant formation of S_2^+ from CS_2 [26–28], so there are apparently no ionic states at suitable energy with long enough lifetimes to explore this remote part of the phase space. The least abundant observed product is O^+, which is seen only above the atomisation threshold at 28 eV.

4.2. Behaviour of individual ionic states

4.2.1. A state (15.07–16 eV)

The first state energetically capable of dissociation is $A\ ^2\Pi$, whose lower vibrational levels can decay

Table 2
Branching from the inner-valence states of OCS^+

Band	C^+	O^+	CO^+	S^+	CS^+
19 eV [a]	···	···	36 ± 2	54 ± 2	2 ± 0.5
23 eV	···	···	46 ± 2.5	41 ± 2.5	11 ± 1.5
26 eV	7 ± 1	0.9 ± 0.3	15 ± 1.5	53 ± 3	21 ± 2
30.4 [b]	21 ± 2	5 ± 1	6 ± 1	51 ± 3	3 ± 1
36 [b]	6.5 ± 1	5 ± 1	23 ± 1	52 ± 2	1 ± 0.5

[a] Across the 19 eV band the yields of CO^+ and CS^+ rise relative to S^+; the figures given are for the centre of the band at 19.9 eV.

[b] A 6% yield of OCS^{2+} is also recorded in the range of these bands.

Table 3
Selected dissociation limits for OCS^+

Fragments	Energy/eV
CO ($X\ ^1\Sigma^+$) + S^+ (^4S_u)	13.52
CO ($X\ ^1\Sigma^+$) + S^+ (^2D_u)	15.36
CO ($X\ ^1\Sigma^+$) + S^+ (^2P_u)	16.56
CO^+ ($X\ ^2\Sigma^+$) + S (^3P_g)	17.17
CO^+ ($X\ ^2\Sigma^+$) + S (^1D_g)	18.32
CS^+ ($X\ ^2\Sigma^+$) + O (^3P_g)	18.56
CO^+ ($A\ ^2\Pi$) + S (^3P_g)	19.73
CS^+ ($A\ ^2\Pi$) + O (^3P_g)	19.99
CS ($X\ ^1\Sigma^+$) + O^+ (^4S_u)	20.44
CS ($X\ ^1\Sigma^+$) + O^+ (^4S_u)	23.76
SO ($A\ ^3\Pi$) + C^+ (^2P_u)	20.17
SO ($X\ ^3\Sigma^-$) + C^+ (^2P_u)	24.92

only to ground state products S^+ (^4S) + CO, whereas for levels above 15.36 eV the excited products S^+ (^2D) + CO are also energetically accessible. For the (000) level we find 21.6% ± 7.6% OCS^+ (and 78.4 ± 14.6% S^+). This result is consistent with the previous result of 17% OCS^+ from fluorescence yield [21]; disagreement with the previous PEPICO value of −3.5% ± 11% OCS^+ [18] is only apparent, because (000) was not resolved from higher vibrational levels in that work. The KERDs from dissociation of levels of *A* below 15.36 eV indicate, in agreement with the TPEPICO results [19], that the CO fragment is formed in a range of vibration levels from $v = 2$ to $v = 6$ with higher vibrational levels favoured. The KERDs for dissociations from levels above 15.4 eV include a wide range of energies, but with a notable increase in the intensity of the low energy component. The simplest explanation is that although dissociation still takes place to the lower limit, an increasing fraction of the products is electronically excited, in agreement with conclusions from the early PEPICO work [18]. Dissociation to very high vibrational levels of ground state products, as proposed by Hubin-Franskin et al. [19], is not ruled out, but represents a less natural explanation. The TOF peaks for S^+ taken from three energy ranges in the band are given in Fig. 6, clearly showing the increasing prominence of low energy releases at the higher excitation energies. The TOF peak taken from the highest range, 15.7 to 15.88 eV, appears from its narrow profile to result from the lower KE fragment ions only, and thus to be due to dissociation mainly to excited fragments.

4.2.2. B state (16.04–16.54 eV)

The peak widths and deduced KERDs change smoothly as the *B* state is reached, suggesting that the breakdown behaviour of OCS^+ in the *B* state is more or less continuous with that of the *A* state. Dissociation seems to go to both accessible limits but mainly to formation of S^+ (^2D) + CO, with a wide range of vibrational levels populated. As in the case of the *A* state, the KERDs could represent formation of ground state products with very high vibrational excitation of the CO, but we consider this less likely. The experimental KERDs themselves are consistent with those of Hubin-Franskin et al. [19] and of Frey et al. [18].

4.2.3. C state (17.96–19.04 eV)

OCS^+ ions in all levels of this state are energetically able to reach three dissociation limits for S^+ and one for CO^+; for the highest vibrational levels a second CO^+ limit is accessible (Table 3). The relative yields of CO^+ and S^+ change notably from one vibrational level to another, as seen in Fig. 4. The kinetic energy release distribution in S^+ formation from *C*(000), Fig. 8, contains weak high energy components (3–4 eV) corresponding to ground state products, and also more intense lower energy components (0–2 eV) which may correspond to ground or excited state S^+ fragment ions. The distribution cannot be interpreted in detail because of the many possible pathways and low energy resolution. In CO^+ formation from $C\ ^2\Sigma^+(000)$ there is a well-defined bimodal KERD, with energy releases of 0.8 and 0.6 eV; by comparison with the available energy of 0.8 eV these show that the CO^+ is formed in $v = 0$ and $v = 1$ only.

4.2.4. Band around 19.9 eV

Holland and MacDonald [16] were unable to provide an unambiguous assignment of this band because the theoretical spectra [14,29] provide insufficient guidance. The main product ions, S^+ and CO^+, are formed in almost equal quantities at most energies within the band. A small yield of CS^+ is also recorded

above 19.5 eV (lowest asymptotic limit 18.53 eV), increasing to 5% ± 1% at 20.5 eV. The ion peak shapes for the major products (Fig. 7) are symmetrical; their widths and shapes indicate broad KERDs with energy releases ranging from 0.2 to 2 eV. This band represents the only states of OCS^+ at energies below 21.2 eV which are energetically capable of producing CO^+ ($A^2\,\Pi$) as a fragment (Table 3). Since emission from this excited fragment is seen in 58.4 nm photoionisation [30] and in helium flowing afterglows [31] with OCS, the low kinetic energy releases in CO^+ formation must correlate with formation of this electronically excited product ion.

4.2.5. Band at 23 eV

The band at 23 eV is well defined in our HeII spectra, as also in the spectra of Holland and MacDonald [16] at a range of photon energies. The theoretical spectra [14,29] suggest two possible origins, either as a 2π satellite or as a 7σ satellite. The overall branching ratios are 46% CO^+, 41% S^+, and 11% CS^+. The onset of significant CS^+ intensity is close to the start of this band. The peak shapes for both S^+ and CO^+, shown in Fig. 7, are forward/backward asymmetric in complementary senses, showing preferential electron emission from the S end of the molecule. The dissociation must be very rapid after ionisation, and as complementary asymmetries are produced, the same state or states probably dissociate into both product channels. No KERDs can be derived, but the main energy releases are of about 2 eV for both ionic products.

4.2.6. Band at 26 eV

In this energy region, which may not really qualify as a separate band, there is only very weak production of CO^+, but continued formation of CS^+ as well as S^+ and a small contribution from C^+ following the atomisation onset. The ion peak shapes seem to be forward/backward symmetric, but the statistics are poor and no reliable KERDs can be derived.

4.2.7. Double ionisation region, 30 to 41 eV

There are two rather indistinct bands at 30.4 and 35.7 eV reported by Holland and MacDonald [16] which are seen best at shorter ionising wavelengths, but the major process in this energy region at 40.8 nm wavelength is double photoionisation. Because we measure the energy of only one of the two electrons ejected in double photoionisation, no definite identification of initial OCS^{2+} states can be made. Rather, the coincident photoelectron spectrum for a doubly charged product such as OCS^{2+} (Fig. 5) is roughly equivalent to a yield curve in photoionisation mass spectrometry. In addition to the doubly charged ion OCS^{2+} we have also measured the yield of $CO^+ + S^+$ ion pairs as electron–ion–ion triple coincidences. From comparison of the yield curves with the known ion collection efficiency and a small correction for loss of sideways-flying ions, it seems that all the CO^+ formed above 32 eV is in the form of such ion pairs. Since S^+ is slightly more abundant than CO^+ at these energies, not all of its formation can be accounted for in this way. The kinetic energy release in cation pair formation is large, about 6 eV; it is consistent with previous measurements of the dissociative double ionisation made by the PEPICO technique with unanalysed electrons [32]. At an electron energy near zero there is a strong photoelectron intensity peak which shows up in all fragment ion channels and especially in the yield of $CO^+ + S^+$ ion pairs. This may possibly be an artefact, but may indicate an indirect ionisation process via neutral or ion state(s) almost matching the photon energy.

5. General discussion and conclusions

It is satisfying that the prediction which led to our investigation of OCS is borne out by the discovery of a band showing an orientation of fragment ions relative to photoelectrons. This is a small additional piece of evidence for a general expectation that photoelectron-fragment ion distributions should usually be anisotropic (contrary to the almost universal practical assumption of isotropy). Our present experimental and analysis methods detect anisotropy only where it is large because of very rapid dissociation, but because anisotropy is never totally abolished by

free rotation, smaller but real anisotropies may be present in most cases.

The particular case of emission from the S end of the OCS molecule in the 23 eV inner valence band may be an example where fixed-molecule angular anisotropy helps with spectral assignment. According to Holland and MacDonald [16], the band is either a 2π or 7σ satellite. These two orbitals differ quite markedly in their Mulliken populations [33], 2π being located mainly on the O atom with very little S character, whereas 7σ is located mainly on S and hardly at all on O. Emission preferentially from the S end of the molecule seems to favour the 7σ assignment, though there is no strict theoretical connection between orbital population and emission direction. Several other states of predominant 7σ character are predicted between 25 and 30 eV, but no forward backward asymmetry could be detected in that range with the present sensitivity.

References

[1] D. Dill, J. Chem. Phys. 96 (1976) 1130.
[2] K.G. Low, P.D. Hampton, I. Powis, Chem. Phys. 100 (1985) 401.
[3] N. Chandra, J. Chem. Phys. 89 (1988) 5987.
[4] D.J. Reynolds, E.H. Van Kleef, I. Powis, J. Chem. Phys. 95 (1991) 8895.
[5] J.H.D. Eland, E.J. Duerr, Chem. Phys. 229 (1998) 1; ibid. 229 (1998) 13.
[6] D.W. Turner, C.W. Brundle, Int. J. Mass Spectrom. Ion Phys. 2 (1969) 195.
[7] B. Kovac, J. Chem. Phys. 78 (1983) 1684.
[8] L.S. Wang, J.E. Ruett, Y.T. Lee, D.A. Shirley, J. Chem. Phys. 47 (1988) 167.
[9] G.H. Fatahallah, A.W. Potts, J. Phys. B 13 (1980) 2545.
[10] J. Delwiche, M.-J. Hubin-Franskin, G. Caprace, P. Natalis, J. Electron Spectrosc. Relat. Phenom. 21 (1980) 205.
[11] R. Frey, B. Gotchev, W.B. Peatman, H. Pollak, E.W. Schlag, Int. J. Mass Spectrom. Ion Phys. 26 (1978) 137.
[12] J. Delwiche, M.-J. Hubin-Franskin, P.-M. Guyon, I. Nenner, J. Chem. Phys. 74 (1981) 4219.
[13] A.W. Potts, T.A. Williams, J. Electron Spectrosc. Relat. Phenom. 3 (1974) 3.
[14] J.P.D. Cook, M.G. White, C.E. Brion, W. Domcke, J. Schirmer, L.S. Cederbaum, W. Von Niessen, J. Electron Spectrosc. Relat. Phenom. 22 (1981) 261.
[15] M.G. White, K.T. Leung, C.E. Brion, J. Electron Spectrosc. Relat. Phenom. 23 (1981) 127.
[16] D.M.P. Holland, M.A. MacDonald, Chem. Phys. 144 (1990) 279.
[17] J.H.D. Eland, Int. J. Mass Spectrom. Ion Phys. 12 (1973) 389.
[18] B. Brehm, R. Frey, A. Küstler, J.H.D. Eland, Int. J. Mass Spectrom. Ion Phys. 13 (1974) 251.
[19] M.-J. Hubin-Franskin, J. Delwiche, P.-M. Guyon, M. Richard-Viard, M. Lavolee, O. Dutuit, J.-M. Robbe, J.-P. Flament, Chem. Phys. 209 (1996) 143.
[20] J.P. Maier, F. Thommen, Chem. Phys. 51 (1980) 319.
[21] D. Klapstein, J.P. Maier, Chem. Phys. Lett. 83 (1981) 590.
[22] U. Boesl, R. Weinkauf, C. Weickhardt, E.W. Schlag, Int. J. Mass Spectrom. Ion Phys. 131 (1994) 87.
[23] T. Field, J.H.D. Eland, Meas. Sci. Technol. 9 (1998) 922.
[24] W.C. Wiley, I.H. McLaren, Rev. Sci. Instrum. 26 (1955) 1150.
[25] Unpublished work, this laboratory.
[26] J.H.D. Eland, J. Berkowitz, J. Chem. Phys. 70 (1979) 5151.
[27] B. Brehm, J.H.D. Eland, R. Frey, A. Küstler, Int. J. Mass Spectrom. Ion Phys. 12 (1973) 213.
[28] D. Mathur, G.R. Kumar, C.P. Safvan, F.A. Rajgara, J. Phys. B: At. Mol. Opt. Phys. 27 (1994) L603.
[29] H. Nakatsuji, Chem. Phys. 76 (1983) 283.
[30] T. Field, J.H.D. Eland, Chem. Phys. Lett. 197 (1992) 542.
[31] M. Tsuji, H. Obase, M. Matsuo, M. Endoh, Y. Nishimura, Chem. Phys. 50 (1980) 195.
[32] S. Hsieh, J.H.D. Eland, J. Phys. B: At. Mol. Opt. Phys. 30 (1997) 4515.
[33] T.X. Carroll, D.E. Ji, T.D. Thomas, J. Electron Spectrosc. Relat. Phenom. 51 (1990) 471.